Research

Ecography 32: 468–480, 2009
doi: 10.1111/j.1600-0587.2008.05512.x

Subject Editor: Jane Elith. Accepted 3 September 2008

Satellite image texture and a vegetation index predict avian biodiversity in the Chihuahuan Desert of New Mexico

Véronique St-Louis, Anna M. Pidgeon, Murray K. Clayton, Brian A. Locke, Dallas Bash and Volker C. Radeloff

V. St-Louis (vstlouis@wisc.edu), A. M. Pidgeon and V. C. Radeloff, Dept of Forest and Wildlife Ecology, Univ. of Wisconsin – Madison, 1630 Linden Dr., Madison, WI 53706, USA. – M. K. Clayton, Dept of Statistics, Univ. of Wisconsin – Madison, 1220 Medical Sciences Center, 1300 University Ave., Madison, WI 53706, USA. – B. A. Locke and D. Bash, Directorate of Environment, Bldg 624, Pleasonton Rd., Fort Bliss, TX 79916, USA.

Predicting broad-scale patterns of biodiversity is challenging, particularly in ecosystems where traditional methods of quantifying habitat structure fail to capture subtle but potentially important variation within habitat types. With the unprecedented rate at which global biodiversity is declining, there is a strong need for improvement in methods for discerning broad-scale differences in habitat quality. Here, we test the importance of habitat structure (i.e. fine-scale spatial variability in plant growth forms) and plant productivity (i.e. amount of green biomass) for predicting avian biodiversity. We used image texture (i.e. a surrogate for habitat structure) and vegetation indices (i.e. surrogates for plant productivity) derived from Landsat Thematic Mapper (TM) data for predicting bird species richness patterns in the northern Chihuahuan Desert of New Mexico. Bird species richness was summarized for forty-two 108 ha plots in the McGregor Range of Fort Bliss Military Reserve between 1996 and 1998. Six Landsat TM bands and the normalized difference vegetation index (NDVI) were used to calculate first-order and second-order image texture measures. The relationship between bird species richness versus image texture and productivity (mean NDVI) was assessed using Bayesian model averaging. The predictive ability of the models was evaluated using leave-one-out cross-validation. Texture of NDVI predicted bird species richness better than texture of individual Landsat TM bands and accounted for up to 82.3% of the variability in species richness. Combining habitat structure and productivity measures accounted for up to 87.4% of the variability in bird species richness. Our results highlight that texture measures from Landsat TM imagery were useful for predicting patterns of bird species richness in semi-arid ecosystems and that image texture is a promising tool when assessing broad-scale patterns of biodiversity using remotely sensed data.

Biodiversity is declining rapidly due to human land-use (Vitousek 1994). Half of the world's bird and mammal species are expected to become extinct in the next 200–300 yr (Smith et al. 1993). Predictive modeling of patterns of biodiversity is thus becoming increasingly important to develop better conservation strategies and to focus management efforts in critical areas, yet, adequately quantifying predictors of biodiversity at broad spatial scales remains challenging. According to MacArthur's (1972) theory of biodiversity, the main drivers of biodiversity include habitat structure, productivity, and climatic stability (MacArthur 1972). The long- and short-term consequences of changes in habitat structure (i.e. here defined as fine-scale spatial variability in plant growth forms) and plant productivity (i.e. amount of green biomass), on patterns of biodiversity are not well understood. There is currently a need for tools that are concurrently flexible (i.e. suitable for a variety of ecosystems) and powerful (i.e. strong predictors) for quantifying habitat structure and plant productivity. To address this need, we present an approach for predicting the spatial patterns of species biodiversity based on the analysis of image texture and vegetation indices derived from remotely sensed data.

To develop appropriate methods for predicting biodiversity, scientists first need to understand the effects of the main drivers of biodiversity, namely climate stability, habitat structure, and plant productivity (MacArthur 1972). Here, we focused on two of those drivers: habitat structure and plant productivity. Climatic stability, as implied by MacArthur (1972), occurs at a much broader spatial and temporal scale than the scope of our analysis so we will not discuss it further. The positive relationship between habitat structure and species diversity has been shown for birds (MacArthur and MacArthur 1961, Wilson 1974, Roth 1976, Luoto et al. 2004), butterflies (Kerr et al. 2001), and mammals (Kerr and Packer 1997), among other taxa. The relationship between biodiversity and productivity can take multiple functional forms (unimodal, increasingly or

decreasingly linear), and is scale dependent (Waide et al. 1999, Chase and Leibold 2002). In some cases where species require scarce resources, species richness is high where plant productivity is high (MacArthur 1972). However, the opposite pattern may also occur where high productivity results in low species richness (Huston 1979). The unimodal relationship between species diversity and productivity has been mainly attributed to competitive exclusion, i.e. a decline in species diversity as one resource becomes dominant over others, accompanied by a reduction in habitat structure (MacArthur 1972). There are other reasons why species diversity in natural systems might be perceived as decreasing at high productivity. If the sampling is biased towards high-productivity habitats of restricted extent, for example, the species/area curve (Gleason 1922) would predict lower diversity in these small areas despite their higher productivity (Abrams 1995). Also, high-productivity areas are often located at the extreme of geographical gradients, where species diversity may be lower because these areas receive immigrants from only one direction, as opposed to areas at intermediate productivity that receive species from either sides of the gradients (Abrams 1995).

Predictive models of biodiversity patterns are important for conservation, and are based on known relationships between predictors quantified at a variety of spatial scales, and empirical data on biodiversity. Quantifying broad-scale predictors is challenging, but remote sensing technologies offer a wide array of tools for doing so (see Nagendra 2001, Turner et al. 2003, Gottschalk et al. 2005, and Leyequien et al. 2007 for extensive reviews). The use of remotely-sensed data in habitat modeling studies has increased substantially in recent years for a wide range of taxa from plants (Zimmermann et al. 2007), to wildlife species (Osborne et al. 2001), and we suspect that it will continue to rise as these data become more widely available. Strong knowledge of the pros and cons of different approaches used for extracting habitat attributes from satellite imagery, especially when the ultimate goal is habitat mapping for one or for a combination of species, is thus becoming increasingly important.

Methods for monitoring biodiversity using remote sensing have in the past been based primarily on deriving habitat suitability maps from classified imagery. In this technique habitat attributes derived from landcover maps (e.g. proportion cover of a given class) are linked with on-the-ground biodiversity data (e.g. number of species in a given area). In a boreal agricultural-forest mosaic, for example, landscape indices derived from classified imagery are good predictors of avian species richness (Luoto et al. 2004). In the Mediterranean region, landscape structure (measured by the authors as the density of land-cover types, the relative proportion of land uses, and the density of patches derived from a landcover map) accounts for a high proportion of the variability in the richness of birds, amphibians, reptiles, and lepidopterans in the landscape (Atauri and Lucio 2001). Landcover classification coupled with information on home ranges shows promise for building habitat suitability maps, and assessing biodiversity distribution (e.g. Florida GAP project, Pearlstine et al. 2002). These examples represent only a few among many cases in which classified imagery was used for mapping habitat suitability, and for understanding broad-scale patterns of biodiversity.

The use of discrete habitat classes for predicting patterns of biodiversity has limitations in some ecosystems, however, for three reasons. First, image classification ignores within-habitat variability. The use of discrete habitat classes thus may not capture characteristics that are important for the species under study, especially if the species distribution is spatially heterogeneous within a given habitat class (Palmeirim 1988). Habitat features (e.g. landscape composition and configuration) obtained from discrete cover classes are sensitive to classification errors (Wagner and Fortin 2005) which may occur more frequently in highly heterogeneous habitats. Second, the arbitrary delineation of boundaries between habitats in ecosystems with broad ecotones may lead to an erroneous image classification at these transition zones. Lastly, habitat classes available from the classification might not reflect the ecological requirements of the organism under study. Semi-arid ecosystems are often characterized by high within-habitat variability and gradual boundaries between habitats (e.g. two adjoining grassland types). The use of traditional image classification methods for assessing patterns of biodiversity is, therefore, particularly limited in semi-arid areas. An alternative that addresses these drawbacks is the use of raw, unclassified imagery (Nagendra 2001).

Two of the three main drivers of biodiversity, habitat structure and productivity, can be potentially assessed using raw remotely sensed data. Habitat structure can be quantified with image texture measures, which are defined as the variability of pixel values in a given area (Haralick et al. 1973). Variability in reflectance values among neighboring pixels can be caused by horizontal variability in plant growth forms. Texture measure can thus function as a surrogate for habitat structure. The textural characteristics of an image depend on the spatial resolution of the imagery and on the features of interest (e.g. trees) (Woodcock and Strahler 1987). At very high spatial resolution, image texture may capture variability in individual shrub species, whereas at lower resolution it may capture variability in the broad distribution of resources (e.g. areas of dense shrubs interspersed with grasses). First-order texture measures such as coefficient of variation in satellite reflectance data are good proxy for landscape diversity (quantified using measures of number of land-cover types, evenness, and topographic index) ($r = 0.67$, $p < 0.0001$) (Rey-Benayas and Pope 1995). Only a few studies have incorporated image texture in predictive models of biodiversity, but their results show promise. In a semi-arid ecosystem of New Mexico, measures from high-resolution digital orthophotos account for up to 56% of the variability in bird species richness; there is a clear positive association between image texture and bird species richness (St-Louis et al. 2006). Image texture obtained from widely available moderate-resolution Landsat Thematic Mapper data can also be used for habitat modeling. Image texture calculated from the variance in the normalized difference vegetation index (NDVI) values in 7×7 pixels is useful, for example, for explaining the occurrence of seven bird species (e.g. song sparrow *Melospiza melodia*, yellow warbler *Dendroica petechia*, black-throated green warbler *Dendroica virens*) in Maine (Hepinstall and Sader 1997). These authors interpret high texture in NDVI as an indication of high variability in habitat types. Species that showed a positive association with image texture are associated with mixed habitats.

Image texture has also the potential of greatly improving habitat suitability models. In a study of the endangered greater rhea *Rhea americana* in Argentina, Bellis et al. (in press) showed that image texture was crucial for distinguishing subtleties within grassland types that influence habitat suitability for that species. Measures that capture habitat heterogeneity (e.g. second-order variance) were better for modeling the occurrence of this species than measures that quantify the uniformity of pixel elements (e.g. angular second moment) (Bellis et al. in press). The aforementioned studies, and others that have used various measures of texture for quantifying wildlife habitat (Knick and Rotenberry 2000, Tuttle et al. 2006, Stickler and Southworth 2008), all show the potential of image texture for predicting biodiversity patterns. However, our understanding of the predictive ability of texture measures in different environments is still limited, and several of the texture measures originally proposed by Haralick et al. (1973) have yet to be tested for ecological analysis. To address these shortcomings, we evaluate and compare the usefulness of several measures of image texture derived from 30-m resolution Landsat TM imagery for predicting patterns of bird species diversity in semi-arid shrub- and grasslands.

In addition to tools for monitoring habitat structure, remote sensing images also allow quantifying plant productivity using vegetation indices. The NDVI, for example, calculated from the red and near infrared bands of the electromagnetic spectrum, measures the amount of photosynthetically active biomass of plant canopies (Tucker 1979). There is a positive correlation ($r = 0.43$–0.81) between net primary productivity (e.g. plant biomass) and vegetation indices such as NDVI calculated from advanced very high resolution radiometer (AVHRR, Schloss et al. 1999). In ecosystems with low vegetation cover, there is a strong relationship between the soil-adjusted vegetation index (SAVI; Huete 1988) and grassland vegetation (Purevdorj et al. 1998). Productivity, as measured by mean NDVI or SAVI, has strong potential for habitat modeling. It has been used in many ecosystem types for modeling species occurrence (Osborne et al. 2001, Laurent et al. 2005) or biodiversity (Hawkins et al. 2003, Seto et al. 2004, Evans et al. 2006). Texture of NDVI, as opposed to mean NDVI only, also accounts for up to 65% of the variability in plant species richness in the Canadian Arctic (Gould 2000). To our knowledge, no studies have yet combined image texture and vegetation indices for modeling biodiversity, even though these two measures are powerful surrogates for habitat structure and plant productivity, and thus important predictors of biodiversity.

The main objective of this research was to evaluate the usefulness of measures of habitat structure and productivity derived from satellite imagery for predicting patterns of bird species richness in semi-arid ecosystems. Specifically, we 1) derived first- and second- order texture measures from unclassified Landsat TM data and one vegetation index (NDVI), 2) compared the predictive ability of measures of habitat structure, and 3) evaluated the increase in ability to predict bird species richness gained from combining measures of habitat structure and measures of plant productivity. We expected to find positive relationships between species richness and both habitat structure and productivity. We also expected that the near infrared TM band (NIR) would be particularly good at predicting bird species richness because of its high sensitivity to photosynthetically active vegetation.

Methods

Study area

Our study was conducted on 282 500 ha of the Chihuahuan Desert of New Mexico, specifically on the McGregor Range of Fort Bliss Military Reserve (Fig. 1). Climate is arid, with average minimum and maximum temperatures ranging from 11 to 19°C and 30 to 35°C respectively for the May–July time period (Western Regional Climate Center 2005). Monthly precipitation ranges between 13 and 44 mm for these months.

Variability in elevation (ranging from 1163 to 2332 m a.s.l.), precipitation, and soil types across the Range determine the plant communities (Dick-Peddie 1993). The dominant soil types include sand, loam, gravel, limestone, and sandstone. For a more complete description of the plant associations occurring in these habitats see Pidgeon et al. (2001, 2003). Seven main habitat types were identified in the study area from a classification based on multiple Landsat TM images (Melhop et al. 1996), including four shrublands (creosote, mesquite, sandsage, and whitethorn), two grasslands (black-grama and mesa grassland), and one tree- dominated habitat (pinyon-juniper).

Bird data

Bird data were acquired at forty-two 108 ha plots between 1 May and 7 June 1996 through 1998 (Fig. 1). Plot locations were stratified according to the seven main habitat classes, for a total of six plots located randomly within each class and surrounded by a buffer of at least 50 m of contiguous habitat (Pidgeon et al. 2003). Each plot consisted of a twelve-point, 3×4 grid with the points located 300 m apart (Fig. 1). Points were surveyed for birds four to five times a year by seven trained observers, between 06:00 and 10:00 am, and in conditions with no strong winds or rain. All birds heard or seen during 10-min periods, and within 150 m of each point were recorded. Species richness was calculated for each 108 ha plot as the tally of species recorded from the 4–5 visits across the twelve points. The 3-yr average of species richness was used because there was no significant year effect (repeated measure ANOVA, $F = 0.0423$, p-value $= 0.9586$). We used an average of three years rather than one year only to account for within-year variability even though it was very small.

Image analysis

A Landsat TM scene acquired on 23 June 1996 was used for calculating habitat structure based on image texture, with digital numbers representing gray scale brightness values ranging from 0 to 255. The normalized difference vegetation index (NDVI) was calculated from the red and near infrared (NIR) Landsat TM bands to capture plant

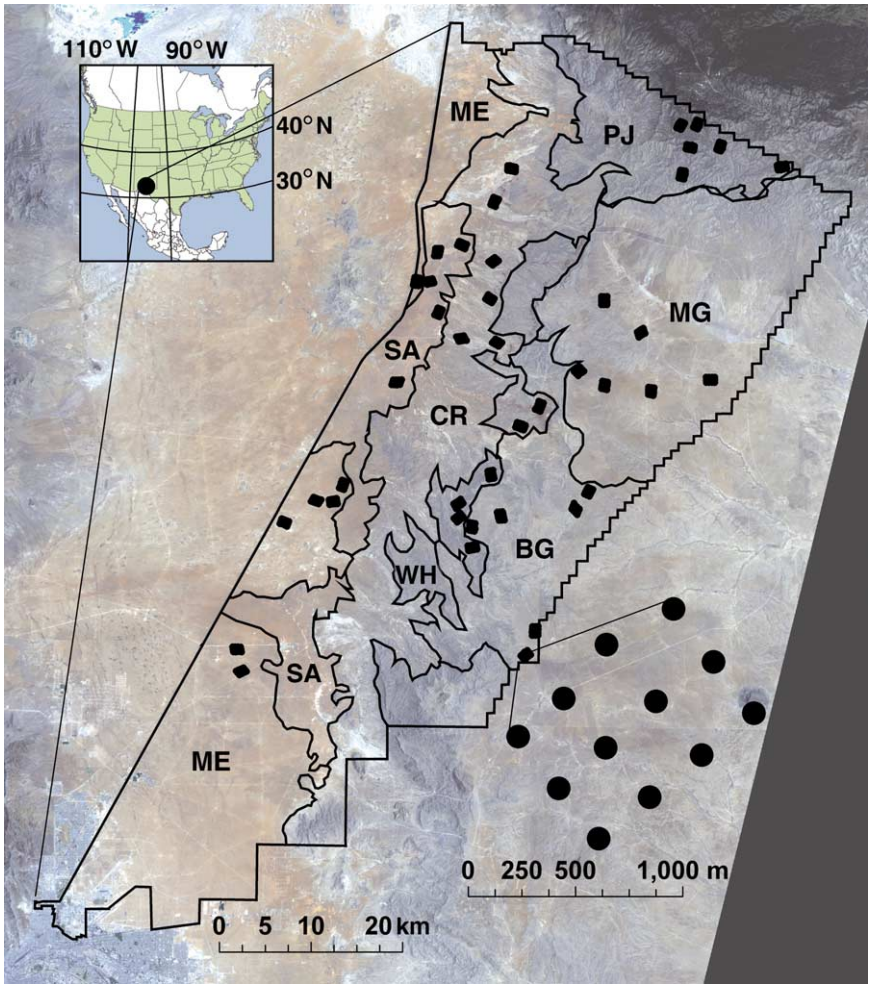

Figure 1. Location of the study sites (black dots) in the McGregor Range of the Fort Bliss military reserve, New Mexico, and an example of a twelve-point 108 ha study grid. The different habitat types are outlined with the bold line, and are defined as follow: BG = black grama, CR = creosote, ME = mesquite, MG = mixed mesa grass, PJ = pinyon-juniper, SA = sandsage, and WH = whitethorn.

productivity. For the purpose of this study, we define plant productivity as the amount of green biomass (i.e. photosynthetically active vegetation) on the ground. Although SAVI is recommended for areas with low vegetation (Huete 1988), preliminary results suggested no substantial differences between the use of NDVI or SAVI for modeling bird species richness in our study area. We therefore used NDVI for completing the analyses presented in this manuscript. All roads were masked prior to the analysis to ensure that we detected texture induced by habitat structure only. Masks were created by digitizing all roads within a plot from USGS digital orthophotos quadrangles (DOQQs; St-Louis et al. 2006).

Two first-order and thirteen second-order texture measures were calculated at each of the 108 ha plots for the six 30-m resolution Landsat TM bands (blue (spectral resolution of 0.45–0.52 μm), green (0.52–0.60 μm), red (0.63–0.69 μm), NIR (0.76–0.90 μm), SWIR-TM5 (1.55–1.75 μm), and SWIR-TM7 (2.08–2.35 μm)) for quantifying habitat structure. Texture of NDVI was also calculated to quantify spatial variability in productivity at each plot. The first-order texture measures used to capture pixel value properties were coefficient of variation and range of reflectance values. Coefficient of variation is defined as the standard deviation of pixel values divided by the mean. Second-order texture measures are calculated from the gray-level co-occurrence matrix (GLCM) and account for the spatial arrangement of pixel values (Haralick et al. 1973). The thirteen second-order statistics used in this analysis include angular second moment, contrast, correlation, difference entropy, difference variance, entropy, inverse difference moment, information measures of correlation 1 and 2, maximal correlation coefficient, sum entropy, sum variance, and sum of squares variance. We omitted Haralick et al. (1973)'s sum average from the analysis because it does not measure spatial variability per se. Two other measures from Haralick's et al. (1973) paper, sum of square variance and sum variance, were also perfectly correlated to one another (Pearson $r = 1$). We therefore randomly chose one of the two for fitting the models (sum variance), reducing the dataset to two first-order and 12 second-order measures of habitat structure (Table 1). Second-order texture measures were calculated in four directions (i.e. from the GLCM computed at 0°, 45°, 90°, and 135°) and averaged. For a complete description of the approach and formulas for calculating second-order texture measures, see Haralick et al. (1973).

Table 1. Abbreviations of the fourteen measures of texture used as proxy for habitat structure.

Type of measures	Abbreviation	Texture measure
First-order measure	cv	Coefficient of variation
	rg	Range
Second-order measures*	asm	Angular second moment
	con	Contrast
	cor	Correlation
	den	Difference entropy
	dva	Difference variance
	ent	Entropy
	icm1 – icm2	Information measure of correlation 1 and 2
	idm	Inverse difference moment
	mcc	Maximal correlation coefficient
	sen	Sum entropy
	sva	Sum variance

*from (Haralick et al. 1973).

Image texture for the six Landsat TM bands, and NDVI was calculated using two approaches for each 108 ha plot: 1) a plot approach, and 2) a within-plot moving window approach. We thereby assessed texture at two spatial scales. The smallest, 0.81 ha (the size of a 3×3 window), corresponds roughly to the home range size of several bird species found in the study area (e.g. ash-throated flycatcher *Myiarchus cinerascens* (territory can be as small as 1 ha (Cardiff et al. 2002)), black-tailed gnatcatcher *Polioptila melanura* (territory size ranges from 0.8 to 2.7 ha per pair (Hensley 1954)), black-throated sparrow *Amphispiza bilineata* (territory can be as small 0.84 ha on average in S Arizona, and 1.61 ha in S New Mexico (Johnson et al. 2002)), or verdin *Auriparus flaviceps* (average territory size is 0.53 ha in two out of three study sites considered by Hensley (1954))). The larger spatial scale, 108 ha, corresponds with the extent of each study plot. We calculated image texture for the plot approach by using all pixel values within the plot. In the within-plot moving window approach, we first ran a 3×3 texture filter across each plot, thus creating 42 images whose pixel values represent the texture calculated in a 3×3 neighborhood (i.e. a total of nine pixels including the middle one). Second, we averaged the resulting image texture values to obtain a plot-level summary statistic of texture. First- and second-order texture measures were computed in Matlab® 7.0.4.365 (TheMathWorks 1984–2005) using the image processing toolbox.

To compare the predictive ability of measures quantified from raw satellite imagery to traditional, classified imagery-based methods for modeling bird species richness, we calculated landscape indices based on a classification obtained from the Southwest regional landcover dataset (USGS National Gap Analysis Program 2004). We first quantified the total number of habitat types within each 108 ha study plot as a measure of habitat richness. We then reclassified the image into two classes (grasslands (hereafter sparse habitat) and shrubland + woodlands (hereafter dense habitat)) (bird species richness is known to vary greatly as a function of vertical diversity provided by shrubs and trees) and quantified the proportion of sparse and dense habitat within each plot, as well as edge density. We expected bird species richness to be positively related with the number of habitat types, edge density, and proportion of dense habitat.

Statistical analyses

Habitat structure and productivity as predictors of species richness

We used Bayesian model averaging to evaluate the relative contribution of measures of habitat structure and plant productivity for determining bird species richness. We fitted four models for each Landsat band as well as for NDVI: 1) a combination of texture measures only (i.e. 14 texture measures) both at the plot and window levels ($struct_p$ and $struct_w$), and 2) a combination of measures of habitat structure and productivity (mean NDVI) at the plot and window levels ($struct_p + prod_p$ and $struct_w + prod_w$). We proceeded this way because we were first interested in comparing the predictive ability of measures of texture alone, and then we wanted to compare the relative contribution of habitat structure and plant productivity for predicting patterns of species richness in our study area. We included quadratic terms for the variables for which including a quadratic term significantly improved (i.e. $p \leq 0.05$) univariate linear models (see Table 2 for a complete list of these variables).

We conducted the Bayesian model averaging analysis using the R package BMA (Raftery et al. 2006). We modified the BMA procedure to consider only models containing up to five predictor variables to prevent overfitting the data. Bayesian information criterion (BIC) values are used to calculate approximate posterior model probabilities for each fitted model (Mi) using the following formula:

$$\Pr(M_i|\text{Data}) \approx \frac{\exp(-\text{BIC}_i/2)\pi_i}{\sum_j \exp(-\text{BIC}_j/2)\pi_j}; \quad (1)$$

Table 2. Plot- and window-level texture measures for which both a linear and a quadratic term were included in the predictive models of bird species richness. We selected these after first fitting both linear and non-linear models between the image textures from Table 1 and bird species richness. Second, we tested for the statistical significance of the quadratic term to evaluate if it should be included (i.e. if the p-value associated with comparing the linear and non-linear model was smaller or equal to 0.05) or not in the predictive models.

Band	Approach	Variable with quadratic term
Blue	Plot	asm, con, rg
	Window	asm, cor, cv, sen
Green	Plot	asm, con, sva
	Window	cor, sva
Red	Plot	con
	Window	con, cor, sva
NIR	Plot	con, sva
	Window	None
SWIR-TM5	Plot	asm, dva, icm2, idm, mcc, sva
	Window	asm, cor, den, dva, ent, icm1, icm2, idm, sen
SWIR-TM7	Plot	asm, den, dva, ent, icm2, idm, mcc, sen
	Window	asm, cor, den, dva, ent, icm1, icm2, idm, sen
NDVI	Plot	asm, con, dva, ent, rg, sva
	Window	con, rg, sva

where π_i is the prior probability for each model (Link and Barker 2006) (1). We chose uniform prior probabilities (1/R; where R is the total number of models fitted) because we had no a priori reason to favor one model over another. Using a method proposed by Madigan and Raftery (1994), a set of parsimonious, data-supported models, is defined using the Occam's window approach with C = 20. This set of models is then used for calculating averaged coefficient estimates with their respective standard deviations (not shown here), and posterior probabilities for each variable (i.e. the probability that a coefficient is different from zero). We used these posterior probabilities as an indication of the relative contribution of each explanatory variable among the set of input variables in the model for explaining bird species richness. To compare the results with traditional classification-based approaches, we also fitted BMA models using the three landscape indices (number of habitat types, edge density, and proportion of dense habitat) calculated within each plot. We did not include proportion of sparse habitat because it was directly related to the proportion of dense habitat.

Residuals of the best predictive models for each band (i.e. smallest σPRESS value) were checked for spatial autocorrelation using semi-variograms at half the maximum distance between study plots.

We used normally distributed errors in our models. While the normality assumption was satisfied in our data (i.e. the residuals showed no departure from normality), we acknowledge that modeling count data using normally distributed errors may lead to negative predictions. Because our focus was not to use these models for on-the-ground mapping of species richness per se, but was rather to evaluate the usefulness of image texture and productivity as a predictive tool, the approach that we took seems appropriate. We must however acknowledge that ecologists interested in direct applications of predictive models (e.g. statistical mapping) should consider using approaches that account for non-normal errors such as Poisson, or other suitable distributions. Useful references to that effect include Jones et al. (2002), Royle et al. (2002), and Sileshi (2006).

Evaluating predictive ability

We used a leave-one-out cross-validation (LOOCV) approach to evaluate the predictive ability of the set of best fitting models (i.e. those selected based on the Occam's window criteria of C = 20). The LOOCV approach was chosen rather than a k-fold approach because of the low number of observations (n = 42). We predicted the value of the ith observation using the regression coefficients obtained by fitting the model leaving the ith observation out. We compared the predictive ability of each fitted model using the standard error of cross-validation prediction calculated as follows:

$$\sigma\text{PRESS}\sqrt{\frac{\sum_{i=1}^{N}(y_i - \hat{y}i)^2}{N - n - 1}} \quad (2)$$

(So and Karplus 1997) where y_i is the value of the ith observation, $\hat{y}_i$ it the predicted value of the ith observation using the reduced model, N = the number of observations (here N = 42), n = the number of predictors in the model (n = 1, 2, 3, 4, or 5 in our case). The numerator in (2) corresponds to the PRESS (predicted residuals sums of squares) statistic (Allen 1974). Here, we chose σPRESS for comparing models rather than raw PRESS values because doing so allows comparing models with different numbers of variables. Small σPRESS values indicate strong predictive ability. For comparison purposes, we calculated the adjusted coefficient of determination ($R^2_{adj.}$) and the BIC for the best predictive models used in the models averaging. All statistical analyses were conducted in R 2.6.0 (R Development Core Team 2007).

Results

Variability in species richness, texture and measures of productivity across habitats

Bird species richness varied greatly across habitats, with lower species richness in grasslands, and higher richness in shrublands and pinyon-juniper. An average of 18 and 19 species occurred in black grama and mesa grasslands respectively. For the four shrublands, an average of 20 species occurred in sandsage, 23 in both creosote and mesquite, and 25 in whitethorn. Species richness was much higher in pinyon-juniper, with 34 species on average.

The variability in reflectance as measured by the first-order coefficient of variation also varied across habitats (Fig. 2). For all bands and for NDVI, the variability was lowest in grasslands. There was a high variability in reflectance values for pinyon-juniper, creosote and whitethorn habitats for most bands. Variability in NDVI values was low in most habitats, except for pinyon-juniper, where it was very high, and whitethorn, where it was intermediate. Mean NDVI values were also very high in the pinyon-juniper habitat compared to the other habitat types.

Habitat structure and productivity as predictors of bird species richness

Because we wanted to evaluate 1) the contribution of multiple measures of habitat structure, and 2) the relative importance of measures of habitat structure versus plant productivity for predicting species richness, we fitted models with texture alone (i.e. models $struct_p$ and $struct_w$), and models that included texture and mean NDVI as a proxy for plant productivity (i.e. models $struct_p + prod_p$ and $struct_w + prod_w$). Measures of habitat structure alone accounted for up to 81.4% (e.g. blue band) of the variability in bird species richness predicted from the six Landsat bands, and up to 82.3% from NDVI (Table 3). Among the six Landsat bands, the predictive ability was higher for the blue, SWIR-TM5, and SWIR-TM7 bands (σPRESS as low as 2.9, 3.5, and 3.6 respectively) than for the three other bands (minimum σPRESS values of 4.2, 4, and 4.8 respectively for the green, red, and NIR bands). The σPRESS values were higher for the NIR band than the five other Landsat bands when habitat structure alone was considered (i.e. up to 5.3), and the models accounted for only up to 46.4% of the variability in species richness.

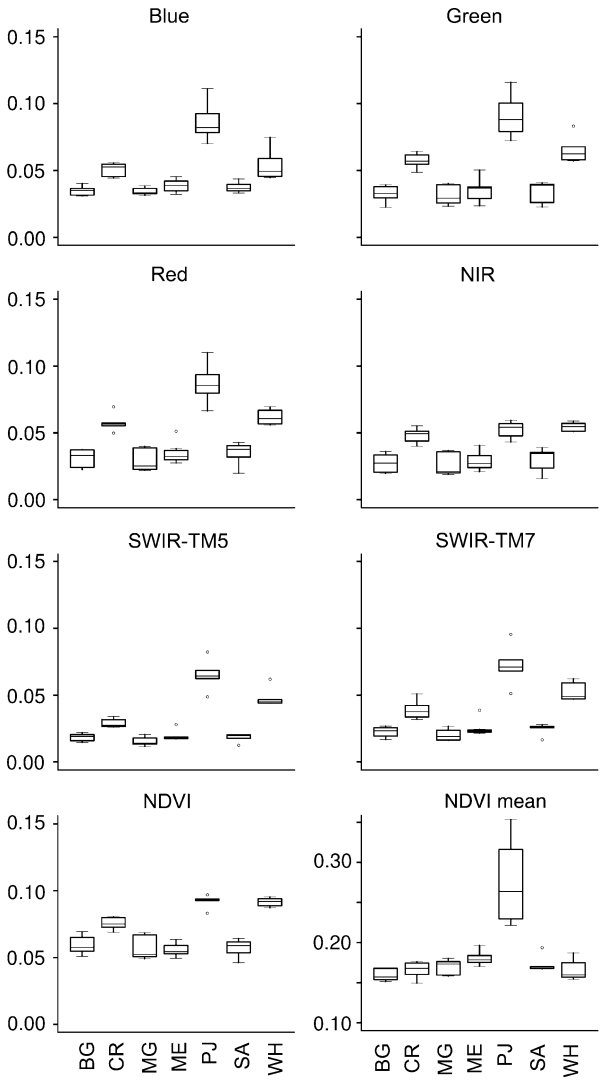

Figure 2. Boxplot of the first-order coefficient of variation values for the six Landsat TM bands and for NDVI across habitat types, and of the mean NDVI values. Coefficient of variation was quantified within a 3×3 filter passed across each plot. The values were then averaged for obtaining a plot-level measurement. The lateral bar represents the median coefficient of variation value across the six plots in each habitat, while the box represents the first and third quantiles and the whiskers indicate the range of the data. Refer to Fig. 1 for habitat type abbreviations.

Models built with the 3×3 window-level data had lower σPRESS values than those build using the plot-level data for all bands except for the SWIR-TM5 band. For NDVI, the results were very similar between the window and plot approach. Preliminary analyses suggest that models built using larger window sizes (e.g. 5×5, and 11×11) showed no substantial improvement over the smallest window size presented here.

Across all measures of habitat structure, first-order coefficient of variation had high posterior probabilities for the blue, green, red, NIR, and SWIR-TM7 (plot level only) bands (Table 4). There was a positive linear relationship between species richness and the green, red, NIR, and SWIR-TM7 bands, and a slightly non-linear relationship with the blue band (Fig. 3). With the exception of a few instances (e.g. high posterior probabilities for difference entropy and difference variance for the blue band at the window level), the other measures of habitat structure had much lower posterior probabilities for these four bands. For the SWIR-TM5 band and NDVI, no measures clearly stood out, with the exception of coefficient of variation in NDVI and NDVI range, both of which had equally high posterior probabilities at the 3×3 window level.

Models that incorporated both measures of habitat structure and plant productivity were better predictive models than models that were based on habitat structure alone (Table 3). The models were very similar across all bands and for NDVI, both in terms of σPRESS (as low as 2.4) and R^2_{adj} values (up to 87.4%), although measures derived from NDVI provided slightly better predictive models. Mean productivity (including its quadratic term) was chosen as a variable in all best fitting models, as shown by its posterior probability of 100% in all cases except for the blue band at the window level (Table 4). Coefficient of variation was the variable with the second highest posterior probability except in the case of the two SWIR bands. For these two bands, no measures had very high posterior probabilities after incorporating productivity in the models. Some individual measures of habitat structure when tested alone accounted for a higher portion of the variability in species richness than mean productivity (e.g. range in NDVI had an R^2_{adj} of 72% as opposed to 61% for mean NDVI) (Fig. 3). However, incorporating mean productivity in the models appears to be important, as shown by its high posterior probabilities across all bands.

For most of the variables that had very high posterior probabilities, the quadratic term (when included) also had high posterior probability (Table 4). Using a strict model selection procedure as described above also resulted in some cases with models that contained a quadratic term but not the corresponding linear term (i.e. when the posterior probability of the quadratic term is higher than that of the linear term). In keeping with the conventional hierarchical principle used for polynomial models (Sokal and Rohlf 1995), for prediction purposes it would be sensible to incorporate a linear term, as well. The variables for which this happened in our study all had very low posterior probabilities, and were therefore most likely weak predictors of bird species richness.

Model diagnostic for the best predictive models of each band and model class (habitat structure only or habitat structure and productivity combined) suggested that the models' assumptions were satisfied, and that there was no spatial autocorrelation in the residuals.

Comparison with classified-imagery based approaches

The models built using landscape indices calculated from a classified image accounted for up to 55% of the variability in bird species richness (Table 5). There was a positive relationship between bird species richness and amount of dense habitat, and also a positive (but not significant according to a 0.95% confidence interval calculated from the estimated coefficient) relationship with both edge

Table 3. Range of R^2_{adj}, BIC, and σPRESS values for the models used to obtain posterior probabilities using the Bayesian average modeling approach. The table presents the results of models containing only measures of habitat structure at the plot ($struct_p$) and window ($struct_w$) levels, and measures of habitat structure and productivity at the plot ($struct_p + prod_p$) and window ($struct_w + prod_w$) levels. The number of models (Nb. mod.) that were used in the model averaging based on the Occam's window criteria of 20 is also indicated.

Band	Model	Nb. mod.	R^2_{adj}	BIC	σPRESS
Blue	$struct_p$	31	45.4–58	249–254	4.7–5.8
	$struct_w$	13	78.8–81.4	214–220	2.9–3.1
	$struct_p + prod_p$	22	74.3–79.1	222–227	3.1–3.5
	$struct_w + prod_w$	11	80.9–83	213–218	2.9–3.3
Green	$struct_p$	33	45.9–54	250–255	4.6–5
	$struct_w$	41	56.2–63.3	242–248	4.2–4.9
	$struct_p + prod_p$	23	77.1–82.4	215–220	2.9–3.1
	$struct_w + prod_w$	15	79.8–82.2	210–215	2.8–3
Red	$struct_p$	22	53.4–56.7	244–250	4.2–4.5
	$struct_w$	41	58.8–67.4	239–243	4–4.3
	$struct_p + prod_p$	22	80.6–84.7	209–214	2.7–2.8
	$struct_w + prod_w$	21	84.4–85.6	203–208	2.6–2.7
NIR	$struct_p$	27	31.5–40.9	259–265	5–5.3
	$struct_w$	40	38.1–46.4	256–262	4.8–5.1
	$struct_p + prod_p$	23	80.3–84.6	209–214	2.7–2.9
	$struct_w + prod_w$	11	84.5–84.9	203–207	2.6–2.7
SWIR-TM5	$struct_p$	42	60.3–72.3	233–238	3.5–4
	$struct_w$	43	63–69.6	233–239	3.7–4
	$struct_p + prod_p$	26	81.7–84.7	206–211	2.6–2.9
	$struct_w + prod_w$	27	82–83.6	207–213	2.7–2.9
SWIR-TM7	$struct_p$	11	55.8–64.6	237–243	3.9–4.2
	$struct_w$	33	60–72.4	233–239	3.6–4.1
	$struct_p + prod_p$	26	83.3–86.1	202–207	2.5–2.7
	$struct_w + prod_w$	26	81–84.1	207–212	2.7–2.8
NDVI	$struct_p$	34	76.4–82.3	213–219	2.8–3.4
	$struct_w$	22	75.8–80.9	217–223	3.1–3.4
	$struct_p + prod_p$	22	85.5–87.4	196–201	2.4–3.2
	$struct_w + prod_w$	26	82.4–86.3	204–209	2.6–2.8

density and the number of habitat types. A coarse classification of the seven main habitat types in the study area accounts for 71.2% of the variability in bird species richness (St-Louis et al. 2006).

Discussion

Adequate understanding and mapping of patterns of biodiversity is crucial to making appropriate management decisions (Debinski and Humphrey 1997). The challenge is to find methodologies to do so at broad-spatial scales, especially in ecosystems with a patchy distribution of resources within habitat classes, where traditional image-classification methods may fail to detect landscape attributes important to biodiversity. Our results suggest that habitat structure and productivity measures derived from unclassified Landsat TM imagery are better predictors of bird species richness in semi-arid ecosystems than landscape indices derived from classified imagery. Assuming that the satellite-derived measures that we used are appropriate surrogates for habitat structure and productivity, our findings support MacArthur's theory (MacArthur 1972) of the important role that these two factors play in determining biodiversity. We found a positive relationship between measures of habitat structure and bird species richness. We speculate that bird species richness is higher in areas of high habitat structure because patches of different plant species, or patches of tall shrubs or trees interspersed with low shrubs or grasses, provide more niches. These areas likely provide a wider variety of resources than low contrast, single-plant species areas. We also found a positive, non-linear relationship between mean productivity and bird species richness. Areas of high plant productivity associated with high biomass contain more foraging resources (Cody 1981) than areas of lower productivity. Variability in productivity was a stronger predictor of bird species richness than mean productivity in our study. This emphasizes again the importance of habitat structure and productivity as two of the main drivers of biodiversity. Our results furthermore highlight the improved power gained by combining measures of habitat structure as well as measures of productivity in predictive models of biodiversity.

The models we obtained using measures of image texture contribute to mounting evidence of the value of image texture for characterizing habitat (e.g. bird territories (Tuttle et al. 2006) and bird occurrence (Hepinstall and Sader 1997)). Our study is one of the first to thoroughly evaluate the usefulness of different measures of texture derived from several spectral bands with the intent of predicting patterns of avian biodiversity. The texture measures that accounted for most of the variability in species richness varied across bands, but some patterns are apparent. There was a positive relationship between first-order coefficient of variation on the blue, green, red, NIR and SWIR-TM7 bands and bird species richness. The coefficient of variation values of all Landsat TM bands was found to vary greatly among habitats in our study area, with high values in pinyon-juniper, to moderate in the shrublands, to low values in the grasslands. From a remote

Table 4. Posterior probabilities of habitat structure and productivity (Prod.) measure resulting from the Bayesian model averaging approach for the models containing only texture measures at the plot ($struct_p$) and window ($struct_w$) levels, and texture measures and mean NDVI also at the plot ($struct_p+prod_p$) and window ($struct_w+prod_w$) levels. The superscript numbers in parenthesis indicate the posterior probabilities for the quadratic term, when it was included in the models (Table 2). The total number of models that were used in the calculation for each band is indicated in Table 3.

		Habitat structure														Prod.
Band	Model	asm	con	cor	cv	den	dva	ent	icm1	icm2	idm	mcc	rg	sen	sva	NDVI
Blue	$struct_p$	$6^{(8)}$	$11^{(8)}$	3	100	54	0	18	16	10	9	5	$28^{(43)}$	20	52	NA*
	$struct_w$	$5^{(0)}$	5	$6^{(5)}$	$100^{(100)}$	95	100	6	12	8	9	7	0	$0^{(5)}$	0	NA
	$struct_p+prod_p$	$8^{(23)}$	$1^{(0)}$	14	69	28	0	12	46	22	10	1	$1^{(1)}$	13	15	$100^{(100)}$
	$struct_w+prod_w$	$3^{(0)}$	0	$3^{(3)}$	$100^{(100)}$	100	100	3	6	4	4	4	0	$0^{(0)}$	0	$33^{(18)}$
Green	$struct_p$	$1^{(4)}$	$12^{(6)}$	5	100	20	1	3	13	2	11	5	28	0	$19^{(31)}$	NA
	$struct_w$	5	2	$40^{(47)}$	100	10	5	8	22	8	11	7	3	9	$4^{(5)}$	NA
	$struct_p+prod_p$	$1^{(0)}$	$5^{(5)}$	0	72	22	0	19	28	13	36	7	0	20	$18^{(4)}$	$100^{(100)}$
	$struct_w+prod_w$	7	6	$6^{(7)}$	98	7	0	7	7	0	2	8	2	0	$6^{(6)}$	$100^{(100)}$
Red	$struct_p$	3	$2^{(5)}$	15	100	9	0	0	12	7	8	11	21	0	13	NA
	$struct_w$	9	$2^{(3)}$	$27^{(75)}$	100	6	3	9	16	9	15	5	3	34	$3^{(5)}$	NA
	$struct_p+prod_p$	8	$0^{(0)}$	2	99	14	8	16	17	8	30	7	14	6	24	$100^{(100)}$
	$struct_w+prod_w$	16	$0^{(0)}$	$5^{(5)}$	100	2	6	10	13	13	4	27	0	9	$0^{(4)}$	$100^{(100)}$
NIR	$struct_p$	3	$7^{(6)}$	10	100	3	5	3	3	4	3	0	57	2	$14^{(21)}$	NA
	$struct_w$	0	12	45	94	30	27	6	8	1	8	1	12	6	9	NA
	$struct_p+prod_p$	2	$23^{(15)}$	3	97	18	3	11	12	5	3	3	36	3	$3^{(10)}$	$100^{(100)}$
	$struct_w+prod_w$	0	7	6	100	6	6	6	6	6	0	6	6	0	7	$100^{(100)}$
SWIRTM5	$struct_p$	$16^{(3)}$	83	5	48	19	$10^{(2)}$	43	14	$4^{(6)}$	$7^{(13)}$	$0^{(0)}$	5	34	$4^{(3)}$	NA
	$struct_w$	$2^{(2)}$	33	$15^{(27)}$	15	$45^{(12)}$	$43^{(8)}$	$1^{(1)}$	$3^{(2)}$	$0^{(0)}$	$2^{(0)}$	4	12	$1^{(1)}$	15	NA
	$struct_p+prod_p$	$5^{(4)}$	0	4	0	27	$6^{(5)}$	11	13	10	$23^{(15)}$	$0^{(0)}$	0	9	$19^{(19)}$	$100^{(100)}$
	$struct_w+prod_w$	$3^{(0)}$	0	$6^{(0)}$	0	$7^{(7)}$	$0^{(2)}$	$9^{(5)}$	$18^{(43)}$	$4^{(8)}$	$10^{(3)}$	10	3	$4^{(5)}$	0	$100^{(100)}$
SWIRTM7	$struct_p$	$3^{(1)}$	8	$4^{(4)}$	91	$9^{(14)}$	$5^{(1)}$	$5^{(2)}$	0	$2^{(2)}$	$18^{(9)}$	$22^{(21)}$	0	$5^{(4)}$	0	NA
	$struct_w$	$7^{(8)}$	2	$3^{(5)}$	23	$5^{(5)}$	$6^{(7)}$	$14^{(14)}$	$72^{(74)}$	$58^{(60)}$	$12^{(19)}$	1	3	$0^{(0)}$	3	NA
	$struct_p+prod_p$	$7^{(2)}$	5	$0^{(7)}$	29	$2^{(6)}$	$6^{(12)}$	$13^{(20)}$	0	$0^{(0)}$	$5^{(4)}$	$0^{(0)}$	33	$15^{(26)}$	0	$100^{(100)}$
	$struct_w+prod_w$	$2^{(0)}$	3	$0^{(0)}$	69	$10^{(11)}$	$7^{(7)}$	$2^{(0)}$	$0^{(0)}$	$0^{(0)}$	$6^{(6)}$	28	20	$6^{(5)}$	7	$100^{(100)}$
NDVI	$struct_p$	$4^{(0)}$	$52^{(50)}$	50	0	20	$6^{(19)}$	$19^{(30)}$	0	0	6	69	$16^{(18)}$	23	$4^{(4)}$	NA
	$struct_w$	0	$9^{(16)}$	32	100	0	9	3	19	7	4	3	$100^{(99)}$	3	$9^{(8)}$	NA
	$struct_p+prod_p$	$7^{(10)}$	$2^{(3)}$	6	99	12	$0^{(0)}$	$10^{(5)}$	5	2	6	15	$0^{(0)}$	2	$6^{(1)}$	$100^{(100)}$
	$struct_w+prod_w$	21	$7^{(16)}$	2	80	2	16	3	27	11	6	17	$3^{(6)}$	15	$3^{(3)}$	$100^{(100)}$

*indicates that mean NDVI was not included in the model.

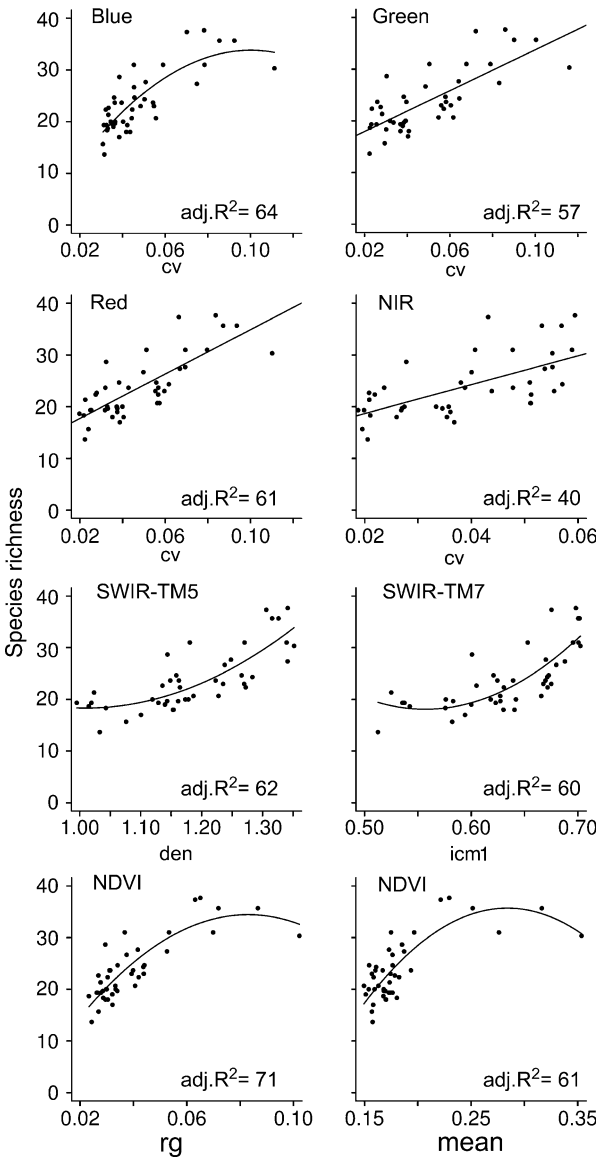

Figure 3. Scatterplot of the relationship between bird species richness and the texture measures at the window level with the highest posterior probability for each band, and NDVI (n = 42). The texture measures represent averages of pixel values obtained in a 3 × 3 filter across each plot. The black line represents result from the linear or non-linear fit. A scatter plot of species richness in relationship with mean NDVI is also shown for comparison. Refer to Table 1 for acronyms' description.

sensing standpoint, this supports previous findings that demonstrated that texture (as measured by local variance) varies as a function of both the size of the objects and the spatial resolution of the image (Woodcock and Strahler 1987). Local variance declines as the size of the object relative to the spatial resolution declines. This may explain why in our study area larger objects (e.g. large mesquite shrubs and pinyon or juniper trees) induce higher texture than objects that were much smaller than the 30 m pixel size of Landsat TM imagery (e.g. scattered yucca in a matrix of grasses). For the SWIR-TM5 band, several texture measures explained bird species richness equally well, as indicated by low posterior probabilities, and high amount of variability explained. The two SWIR-TM bands, sensitive to vegetation moisture content, provide good predictive models for bird species richness. It is possible that mesquite and pinyon-juniper habitats (i.e. two habitats that are associated with high avian species richness) both exhibited high variability in these two bands induced by the interspersion of green, photosynthetically active vegetation with bare ground or grasses (e.g. mesquite dune, juniper or pinyon tree, interspersed with sparse vegetation).

A surprising result was the weak relationship between NIR texture and bird species richness. NIR is primarily sensitive to photosynthetically active vegetation, thus we were expecting a strong relationship between variability in vegetation greenness as captured by NIR and bird species richness. A possible explanation might be that, in the Chihuahuan Desert of New Mexico, there is a very low contrast between soil and vegetation in the NIR wavelength (Franklin et al. 1993). Dry, bright soils can even induce NIR values that are greater than those of the vegetation present (Franklin et al. 1993). However, in the period just preceding Landsat data acquisition the monsoon rains were particularly heavy, with frequent downpours from 15 to 25 June, 2006, and standing water in many low-lying areas (Pidgeon unpubl.). Without more detailed data on rainfall patterns across the study area, it is not possible to truly evaluate what caused the lack of a relationship between NIR texture and bird species richness.

Variability in productivity, measured by NDVI texture, was a better predictor of bird species richness than any of the measures of habitat structure from individual Landsat TM bands. NDVI texture captures heterogeneity in the amount of vegetation (Hepinstall and Sader 1997). High texture can therefore be induced by high horizontal variability among plant growth forms. Habitats that are heterogeneous either in terms of plant species composition, or in terms of the spatial distribution of plants, create multiple niches that bird species can exploit. In our

Table 5. Posterior probabilities and model averaged coefficients (SD) of the landscape indices used for explaining patterns in species richness at the 42 study plots. The R^2_{adj} values of the five models used for the averaging ranged from 52.4 to 55%, while the BIC and σPRESS values ranged from 247–251, and 4.04–4.15 respectively.

Model averaged measure	Amount of dense habitat	Edge density	Number of habitat types
Posterior probability	$100^{(76)*}$	34	21
Averaged coefficient (SD)	Linear term: 0.452 (0.291) Quadratic term: −0.004 (0.003)	0.0162 (0.0514)	0.135 (0.373)

*This value represents the posterior probability obtained for the quadratic term in the models.

study area, high texture was found in the pinyon-juniper habitat, which is characterized by trees of different heights and at different densities, interspersed in a matrix of grasses. Individual bird species may be attracted to areas of heterogeneous plant productivity rather than areas of uniformly high plant productivity for several reasons: 1) movement might be facilitated by a non-uniform distribution of plants (dense plant structure is hard to move through and flying over it exposes birds to avian predators), or 2) bird species that have generalist diets may find more foraging opportunities (several species in this ecosystem forage both on the ground and in shrubs).

The positive relationship that we found between texture in productivity and bird species richness concurs with results from previous studies. At broad spatial scale, there is a positive, linear relationship between bird species richness and areas of high NDVI values (Hurlbert and Haskell 2003, Evans et al. 2006). There is also a strong correlation between NDVI mean, maximum and standard deviation and bird species richness at smaller spatial scales (Seto et al. 2004), although the shape of this relationship (either linear or quadratic) is not clear. Our results suggest that the functional shape of birds' response to increasing mean productivity is non-linear in our study area, with a slight decline in species richness at higher productivity. We found the same pattern with increase in variability in productivity (e.g. range). However, at this point and with only 42 study sites, we cannot claim that the relationship is clearly unimodal because only few data points exhibited high productivity, and the relationship may just plateau at high habitat structure values rather than decline. Further research is needed to determine the functional shape of the relationship between avian biodiversity and productivity in this ecosystem and at the spatial scale of the study.

Because of the low contrast of the NIR band in this ecosystem (Franklin et al. 1993), the strong relationship between NDVI texture and bird species richness might depend more on the red band, which has lower reflectance values where there is high vegetation cover (Franklin et al. 1993). The mean red reflectance value is, in fact, very low for pinyon-juniper habitat in our study area, and higher for the two grassland habitats. In our study, preliminary results suggested that SAVI (with $L = 0.75$) was not substantially better at predicting bird species richness than NDVI. For the purpose of monitoring biodiversity, we can conclude from our results that NDVI is a suitable measure for capturing differences in productivity across habitats in this ecosystem.

Our models suggest that the plot and the within-plot moving window approaches yielded models with very similar predictive ability, but that the moving window approach provided slightly better predictive models than the plot approach for all bands except NDVI. This might be explained by the fact that texture in a 3×3 window represents a spatial scale similar to the territory size of many bird species breeding in the study area (e.g. ash-throated flycatcher, black-tailed gnatcatcher, black-throated sparrow, or verdin).

Models built using combinations of up to five measures of habitat structure and mean productivity from 30 m resolution Landsat TM imagery performed best, and explained up to 87.4% of the variability in bird species richness. In the same study area, we previously demonstrated that single texture measures derived from 1-m resolution digital orthophotos explain up to 57% of the variability in bird species richness (St-Louis et al. 2006). Our results suggest that in this ecosystem, medium resolution images, such as Landsat TM, may be more useful than high-resolution imagery, such as digital orthophotos, for mapping patterns of bird species richness. Even in the visible range (i.e. blue, green, red), it appears that single measures of image texture from 30 m resolution Landsat TM imagery were better predictors of bird species richness than measures derived from 1 m digital orthophotos. This suggests that a 30 m pixel size, although it does not retain information about individual habitat elements that birds might key in on (e.g. individual shrubs), is nonethe-less an appropriate grain for calculating measures of avian habitat structure and productivity.

Despite limitations introduced by our low sample size and lack of independent validation data, our study demonstrates the potential of image texture and productivity indices for predicting patterns of biodiversity in ecosystems characterized by high within-habitat variability. Further studies are needed for evaluating the applicability of these tools in other ecosystems, but many recent examples confirm the potential of these measures for wildlife studies (e.g. Stickler and Southworth 2008, Bellis et al. in press). The use of image texture analysis from satellite imagery for predicting patterns of biodiversity is therefore very promising, and could be applicable in a wide range of ecosystems if supported by adequate ground truthing (Gottschalk et al. 2005).

Conclusion

Remote sensing technologies are increasingly used for understanding and predicting broad-scale patterns of biodiversity. Our results, along with results from previously published studies, suggest that image texture and vegetation indices are promising tools for predicting broad-scale patterns of biodiversity. Use of image texture measures derived from satellite data has potential to provide quick, cost-effective, assessment of biodiversity hotspots in areas not suitable for application of most traditional, classified imagery-based approaches. The main conclusions of our study are twofold: 1) habitat structure, as measured by image texture of Landsat TM bands, explains up to 81.4% of the variability in avian species richness, while habitat structure derived from NDVI explains up to 82.3%, and 2) a combination of measures of habitat structure and productivity explains up to 87.4% of the variability in species richness. Image texture from satellite imagery has been applied successfully in forested ecosystems. Here, we show that image texture from 30 m resolution Landsat TM images is also a strong predictor of bird species richness in semi-arid ecosystems. We also demonstrate the value of combining measures of habitat structure and plant productivity for broad-scale assessments of patterns of avian biodiversity. This work expands our understanding of the range of ecosystems in which image texture and vegetation indices can be used for monitoring broad-scale patterns of biodiversity.

Acknowledgements – We would like to thank all field assistants who collected bird data between 1996 and 1998. Tobias Kuemmerle, two anonymous reviewers, and the subject matter editor, made valuable comments which greatly improved this manuscript. We gratefully acknowledge support by the Strategic Environmental Research and Development Program. Support for acquiring bird data was provided by the U.S. Dept of Defense Legacy Resource Management Program, Ft. Bliss Directorate of Environment, USGS BRD Texas Cooperative Fish and Wildlife Research Unit, USGS BRD Wisconsin Cooperative Wildlife Research Unit, the Dept of Wildlife Ecology, and the Dept of Forest Ecology and Management, Univ. of Wisconsin-Madison.

References

Abrams, P. A. 1995. Monotonic or unimodal diversity-productivity gradients: what does competition theory predict? – Ecology 76: 2019–2027.

Allen, D. M. 1974. The relationship between variable selection and data augmentation and a method for prediction. – Technometrics 16: 125–127.

Atauri, J. A. and de Lucio, J. V. 2001. The role of landscape structure in species richness distribution of birds, amphibians, reptiles and lepidopterans in Mediterranean landscapes. – Landscape Ecol. 16: 147–159.

Bellis, L. M. et al. in press. Modeling habitat suitability for the endangered greater rhea *Rhea americana* in central Argentina based on satellite image texture. – Ecol. Appl.

Cardiff, S. W. et al. 2002. Ash-throated flycatcher (*Myiarchus cinerascens*). – In: Poole, A. (ed.), The birds of North America online. Cornell Lab of Ornithology, Ithaca, retrieved from the birds of North America online, <http://bna.birds.cornell.edu/bna/species/664>; doi:10.2173/bna.664.

Chase, J. M. and Leibold, M. A. 2002. Spatial scale dictates the productivity-biodiversity relationship. – Nature 416: 427–430.

Cody, M. L. 1981. Habitat selection in birds: the roles of vegetation structure, competitors, and productivity. – BioScience 31: 107–113.

Debinski, D. M. and Humphrey, P. S. 1997. An integrated approach to biological diversity assessment. – Nat. Areas J. 17: 355–365

Dick-Peddie, W. A. 1993. New Mexico vegetation: past, present, and future. – Univ. of New Mexico Press.

Evans, K. L. et al. 2006. Abundance, species richness and energy availability in the North American avifauna. – Global Ecol. Biogeogr. 15: 372–385.

Franklin, J. et al. 1993. Reflectance of vegetation and soil in Chihuahuan Desert plant communities from ground radiometry using SPOT wavebands. – Remote Sens. Environ. 46: 291–304.

Gleason, H. A. 1922. On the relationship between species and area. – Ecology 3: 158–162.

Gottschalk, T. K. et al. 2005. Thirty years of analyzing and modelling avian habitat relationships using satellite imagery data: a review. – Int. J. Remote Sens. 26: 2631–2656.

Gould, W. 2000. Remote sensing of vegetation, plant species richness, and regional biodiversity hotspots. – Ecol. Appl. 10: 1861–1870.

Haralick, R. M. et al. 1973. Textural features for image classification. – IEEE Trans. Syst. Man Cybernetics SMC-3: 610–621.

Hawkins, B. A. et al. 2003. Energy, water, and broad-scale geographic patterns of species richness. – Ecology 84: 3105–3117.

Hensley, M. M. 1954. Ecological relations of the breeding bird population of the desert biome in Arizona. – Ecol. Monogr. 24: 185–208.

Hepinstall, J. A. and Sader, S. A. 1997. Using Bayesian statistics, Thematic Mapper satellite imagery, and breeding bird survey data to model bird species probability of occurrence in Maine. – Photogr. Eng. Remote Sens. 63: 1231–1237.

Huete, A. R. 1988. A soil-adjusted vegetation index (SAVI). – Remote Sens. Environ. 25: 295–309.

Hurlbert, A. H. and Haskell, J. P. 2003. The effect of energy and seasonality on avian species richness and community composition. – Am. Nat. 161: 83–97.

Huston, M. 1979. A general hypothesis of species diversity. – Am. Nat. 113: 81–101.

Johnson, M. J. et al. 2002. Black-throated sparrow (*Amphispiza bilineata*). – In: Poole, A. (ed.), The birds of North America online. Cornell Lab of Ornithology, Ithaca, retrieved from the birds of North America online, <http://bna.birds.cornell.edu/bna/species/637>; doi:10.2173/bna.637.

Jones, M. T. et al. 2002. Poisson regression: a better approach to modeling abundance data? – In: Scott, J. M. et al. (eds), Predicting species occurrences: issues of scale and accuracy. Island Press, pp. 411–418.

Kerr, J. T. and Packer, L. 1997. Habitat heterogeneity as a determinant of mammal species richness in high-energy regions. – Nature 385: 252–254.

Kerr, J. T. et al. 2001. Remotely sensed habitat diversity predicts butterfly species richness and community similarity in Canada. – Proc. Nat. Acad. Sci. USA 98: 11365–11370.

Knick, S. and Rotenberry, J. T. 2000. Ghosts of habitats past: contribution of landscape change to current habitats used by shrubland birds. – Ecology 81: 220–227.

Laurent, E. J. et al. 2005. Using the spatial and spectral precision of satellite imagery to predict wildlife occurrence pattern. – Remote Sens. Environ. 97: 249–262.

Leyequien, E. et al. 2007. Capturing the fugitive: applying remote sensing to terrestrial animal distribution and diversity. – Int. J. Appl. Earth Obs. Geoinform. 9: 1–20.

Link, W. A. and Barker, R. J. 2006. Model weights and the foundations of multimodel inference. – Ecology 87: 2626–2635.

Luoto, M. et al. 2004. Predicting bird species richness using remote sensing in boreal agricultural-forest mosaics. – Ecol. Appl. 14: 1946–1962.

MacArthur, R. H. 1972. Geographical ecology: patterns in the distribution of species. – Harper and Row.

MacArthur, R. H. and MacArthur, J. W. 1961. On bird species diversity. – Ecology 42: 594–598.

Madigan, D. and Raftery, A. E. 1994. Model selection and accounting for model uncertainty in graphical models using Occam's window. – J. Am. Stat. Assoc. 89: 1535–1546.

Melhop, P. et al. 1996. Vegetation of Fort Bliss, Texas and New Mexico, final report. Volume II; vegetation map. – New Mexico Natural Heritage Program, Biology Dept, Univ. of New Mexico.

Nagendra, H. 2001. Using remote sensing to assess biodiversity. – Int. J. Remote Sens. 22: 2377–2400.

Osborne, P. E. et al. 2001. Modelling landscape-scale habitat use using GIS and remote sensing: a case study with great bustards. – J. Appl. Ecol. 38: 458–471.

Palmeirim, J. M. 1988. Automatic mapping of avian species habitat using satellite imagery. – Oikos 52: 59–68.

Pearlstine, L. G. et al. 2002. Assessing state-wide biodiversity in the Florida Gap analysis project. – J. Environ. Manage. 66: 127–144.

Pidgeon, A. M. et al. 2001 Response of avian communities to historic habitat change in the northern Chihuahuan Desert. – Conserv. Biol. 15: 1772–1788.
Pidgeon, A. M. et al. 2003. Landscape-scale patterns of black-throated sparrow (*Amphispiza bilineata*) abundance and nest success. – Ecol. Appl. 13: 530–542.
Purevdorj, T. et al. 1998. Relationships between percent vegetation cover and vegetation indices. – Int. J. Remote Sens. 19: 3519–3535.
Raftery, A. et al. 2006. BMA: Bayesian model averaging. R package ver. 3.03. – <http://www.r-project.org> <http://www.research.att.com/~volinsky/bma.html>.
R Development Core Team 2007. R: a language and environment for statistical computing. – R Foundation for Statistical Computing, <www.R-project.org>.
Rey-Benayas, J. M. and Pope, K. O. 1995. Landscape ecology and diversity patterns in the seasonal tropics from Landsat TM imagery. – Ecol. Appl. 5: 386–394.
Roth, R. R. 1976. Spatial heterogeneity and bird species diversity. – Ecology 57: 773–782.
Royle, J. A. et al. 2002. Statistical mapping of count survey data. – In: Scott, J. M. et al. (eds), Predicting species occurrences: issues of scale and accuracy. Island Press, pp. 411–418.
Schloss, A. L. et al. 1999. Comparing global models of terrestrial net primary productivity (NPP): comparison of NPP to climate and the normalized difference vegetation index NDVI. – Global Change Biol. 5 (Suppl. 1): 25–34.
Seto, K. C. et al. 2004. Linking spatial patterns of bird and butterfly species richness with Landsat TM derived NDVI. – Int. J. Remote Sens. 25: 4309–4324.
Sileshi, G. 2006. Selecting the right statistical model for analysis of insect count data by using information theoretic measures. – Bull. Entomol. Res. 96: 479–488.
Smith, F. D. M. et al. 1993. Estimating extinction rates. – Nature 364: 494–496.
So, S. S. and Karplus, M. 1997. Three-dimensional quantitative structure-activity relationships from molecular similarity matrices and genetic neural networks. 2. Applications. – J. Med. Chem. 40: 4360–4371.
Sokal, R. R. and Rohlf, F. J. 1995. Biometry: the principles and practice of statistics in biological research, 3rd ed. – W. H. Freeman.
Stickler, C. M. and Southworth, J. 2008. Application of multi-scale spatial and spectral analysis for predicting primate occurrence and habitat associations in Kibale National Park, Uganda. – Remote Sens. Environ. 112: 2170–2186.
St-Louis, V. et al. 2006. Image texture as a predictor of bird species richness. – Remote Sens. Environ. 105: 299–312.
TheMathWorks 1984–2005. Matlab. – Natik, MA, USA.
Tucker, C. J. 1979. Red and photographic infrared linear combinations for monitoring vegetation. – Remote Sens. Environ. 8: 127–150.
Turner, W. et al. 2003. Remote sensing for biodiversity science and conservation. – Trends Ecol. Evol. 18: 306–314.
Tuttle, E. M. et al. 2006. Using remote sensing image texture to study habitat use patterns: a case study using the polymorphic white-throated sparrow *Zonotrichia albicollis*. – Global Ecol. Biogeogr. 15: 349–357.
USGS National Gap Analysis Program 2004. Provisional digital land cover map for the southwestern United States. Version 1.0. – RS/GIS Laboratory, College of Natural Resources, Utah State Univ.
Vitousek, P. M. 1994. Beyond global warming: ecology and global change. – Ecology 75: 1861–1876.
Waide, R. B. et al. 1999. The relationship between productivity and species richness. – Annu. Rev. Ecol. Syst. 30: 257–300.
Wagner, H. H. and Fortin, M.-J. 2005 Spatial analysis of landscapes: concepts and statistics. – Ecology 86: 1975–1987.
Western Regional Climate Center 2005. Orogrande 1N New Mexico. –<http://www.wrcc.dri.edu>, accessed 8 Dec. 2005.
Wilson, M. F. 1974. Avian community organization and habitat structure. – Ecology 55: 1017–1029.
Woodcock, C. E. and Strahler, A. H. 1987. The factor of scale in remote sensing. – Remote Sens. Environ. 21: 311–332.
Zimmermann, N. E. et al. 2007. Remote sensing-based predictors improve distribution models of rare, early successional and broadleaf tree species in Utah. – J. Appl. Ecol. 44: 1057–1067.